where

$$k' = \frac{k_3 k_4}{k_5} [H_2O]$$

The derived rate expression (3) is in good agreement with the experimental results for manganese chloride and manganese sulfate inhibitors. Rate expression (5) satisfies the experimental findings of triethanolamine inhibited runs. From the results shown in Figure 6, we can conclude that the concentration of $[I]$ is directly proportional to the total concentration of the inhibitor present in the reacting solution. Of the two inhibitors, manganese (II) seems to be a better electron transfer reagent in bringing about this inhibition.

The experimental results have shown that the rate decreases with the increase in pH values. It is possible that dithionite undergoes hydrolysis (Bailar et al., 1973) which would partially remove the dithionite ion from the reaction medium, thereby reducing its effective concentration available for oxidation reaction. The higher the concentration of OH ions, that is, increased values of pH ,the greater would be the extent of hydrolysis reaction, resulting in increased depletion of dithionite concentrations and thus decreasing the rate of oxidation effectively.

NOTATION

$[I]$ = inhibitor concentration, mole/l
k_i, k_2, etc. = rate constants for reaction steps
M = concentration, mole/l
$[O_2]$ = average oxygen concentration, mole/l
r = rates, mole/(l)(s), $-d[O_2]/dt$
$[S_2O_4^{--}]$ = average dithionite concentration, mole/l
t = time, s
T = absolute temperature, °K

LITERATURE CITED

Ashmore, P. G., *Catalysis and Inhibition of Chemical Reactions*, Butterworths, London, England (1963).

Bailar, J. C., H. J. Emelus, S. R. Nyholm, and A. F. Trotman Dickeson, "Comprehensive Inorganic Chemistry," Pergamon Press, Oxford, England (1973).

Burlamacchi, L., G. Guarini, and E. Tiezzi, *Trans. Faraday Soc.*, **65**, 496 (1969).

Committee on Analytical Methods Report, "Essay of Sodium Hydrosulfite," *Am. Dye Stuff. Reptr.*, **46**, 443 (1957).

Dean, J. A., *Langas Hand Book of Chemistry*, 11 ed., McGraw-Hill, New York (1973).

Hartridge, H., and F. J. W. Roughton, "Rate of Oxidation and Reduction of Hemoglobin," *Proc. Roy. Soc. (London)*, **A104**, 376 (1923).

Jhaveri, A. S., and M. M. Sharma, "Absorption of Oxygen in Aqueous Alkaline Solutions of Sodium Dithionite," *Chem. Eng. Sci.*, **23**, 1 (1968).

Klemin, N. G., and P. V. Moriganov, "Stability of Solutions of Sodium Hydrosulfite and Leuco Compounds or Brilliant Violet K in Different Media," *Chem. Abs.*, **55**, 9881a (1958).

Lynn, S., Ph.D. thesis, Calif. Inst. Technol. (1954).

———, R. G. Rinker, and W. H. Corcoran, "The Monomerization Rate of Dithionite Ion in Aqueous Solution," *J. Phys. Chem.*, **68**, 2363 (1964).

Mecco, J. M., "High Temperature Vat Dyeing Baths," *Chem. Abs.*, **48**, 11801 (1954).

Meyer, J., *Z. Anorg. Chem.*, **34**, 43 (1903); cited in Rinker et al. (1960).

Mishra, G. C., and R. D. Srivastava, "Kinetics of Oxidation of Ammonium Sulfite by Rapid Mixing Method," *Chem. Eng. Sci.*, **30**, 1387 (1975).

———, "Homogeneous Kinetics of Potassium Sulfite Oxidation," *ibid.*, **31**, 969 (1976).

Morello, J. A., M. R. Craw, H. P. Constantine, and R. E. Forster, "Rate of Reaction of Dithionite Ion with O_2 in Aqueous Solution," *J. Appl. Physiol.*, **19**, 522 (1964).

Nicloux, M., "Oxidation of Sodium Hyposulfite with Free Oxygen," *Chem. Abs.*, **27**, 3160 (1933).

Pinsent, B. R. W., L. Pearson, and F. J. W. Roughton, "The Kinetics of Combination of Carbon Dioxide with Hydroxide Ion," *Trans. Faraday Soc.*, **52**, 1512 (1956).

Rinker, R. G., T. P. Gordon, D. M. Mason, and W. H. Corcoran, "The Presence of SO_2^- Radical Ion in Aqueous Solution of Sodium Dithionite," *J. Phys. Chem.*, **63**, 302 (1959).

———, and R. R. Sakadia, Kinetics and Mechanism of the Oxidation of the Dithionite Ion ($S_2O_4^{--}$) in Aqueous Solution," *ibid.*, **64**, 573 (1950).

Roughton, F. J. W., *Techniques of Organic Chemistry*, Vol. VIII, Interscience, New York (1963).

Srivastava, R. D., A. F. McMillan, and I. J. Harris, "The Kinetics of Oxidation of Sodium Sulfite," *Can. J. Chem. Eng.*, **46**, 181 (1968).

Uri, N., "Inorganic Free Radicals in Solution," *Chem. Rev.*, **50**, 375 (1952).

Washburn, *International Critical Tables of Numerical Data*, Vol. V, p. 201, McGraw Hill, New York (1929).

Manuscript received December 15, 1976; revision received October 24, and accepted November 21, 1977

Adsorption Rate on Molecular Sieving Carbon by Chromatography

KAZUYUKI CHIHARA
MOTOYUKI SUZUKI
and
KUNITARO KAWAZOE

Institute of Industrial Science
University of Tokyo
7-22-1 Roppongi, Minato-ku, Tokyo
106 Japan

Diffusivities in the micropore and adsorption equilibrium constants were determined for neon, argon, krypton, xenon, nitrogen, methane, ethylene, ethane, propylene, propane, n-butane, and benzene on molecular sieving carbon by chromatographic measurement and moment analysis. Isosteric heat of adsorption was found to be 2.6 times heat of vaporization for the gases examined here. Two separate linear relations were obtained between activation energies of diffusion in micropore and isosteric heats of adsorption for rare gases, methane, and benzene, and for n-paraffin and n-olefin except methane.

SCOPE

Diffusion as well as adsorption equilibrium in adsorbent particles is important in designing adsorption processes. The possible mechanisms of diffusion in adsorbent particles are classified into three groups in the case of gaseous adsorption. They are diffusion in gas phase of macropores

such as molecular diffusion or Knudsen diffusion, surface diffusion which occurs in the adsorbed phase, or diffusion in the micropores whose diameters are comparable with molecular diameter of adsorbates. The engineering estimation of the effective diffusivities for the first and second cases is almost possible, but when the intraparticle diffusion is controlled by the third mechanism, there are still some ambiguities in estimating the order of magnitude of the adsorption rate. Molecular sieving materials such as molecular sieving carbon (MSC) and zeolite have micropores of well-defined structure. Micropores of MSC are considered to be slits of about 5Å opening between two graphitized carbon layer planes, while zeolites have network structures. Study of micropore diffusion in molecular sieving materials is significant since they provide fundamental characteristics of diffusion in other adsorbents which possess micropores of wide varieties. Though many investigations for the intracrystalline diffusion in zeolite have been made, there has been, however, little work on diffusion in MSC.

Micropore diffusion of adsorbate molecules occurs in the potential energy field which is due to interactions between adsorbate molecules and adsorbent lattice atoms. This diffusion is generally described as each molecule hopping from one minimum of the potential energy distribution to another, or adsorption site to site, across potential energy barriers which separate adjacent sites. This type of micropore diffusion is a kind of activated process and is called activated diffusion.

The purpose of this work is to experimentally determine the micropore diffusivities and adsorption equilibrium constants of various gases in MSC at wide temperature ranges and to correlate the obtained activation energies of micropore diffusion and isosteric heats of adsorption with the properties of adsorbate gases. Chromatographic measurements were made for this purpose. By introducing the concentration pulse of adsorbate to the carrier gas stream at the inlet of the adsorbent column, the concentration elution curve at the outlet of the column was measured. Adsorption equilibrium constant and micropore diffusivity were determined by means of moment analysis of elution curves.

CONCLUSIONS AND SIGNIFICANCE

Adsorption equilibrium constants increased while diffusivities in micropore decreased at lower temperature as well as with high molecular weight for the rare gases and for the hydrocarbons.

Isosteric heats of adsorption q_{st} which are a measure of interactions between adsorbate molecules and adsorbent lattice atoms were determined from temperature dependency of adsorption equilibrium constants. q_{st} for the hydrocarbons was found to be in a linear relation with the carbon numbers. Also, it was possible to correlate all the data by $q_{st} = 2.6\Delta H$, where ΔH is heat of vaporization of adsorbate.

The isosteric heats of adsorption obtained here were twice as much as those for graphitized thermal carbon black (GTCB). It seems reasonable that heat of adsorption in MSC is twice that of GTCB because molecules adsorbed in micropores of MSC have interactions with the carbon layer planes of both sides, while molecules adsorbed on the surface of GTCB interact with only one carbon layer plane.

Activation energies of diffusion in the micropore of MSC, E, were determined by an Arrhenius' plot of micropore diffusivities for each gas. Diffusion in micropores is activated as was expected because of high values of the activation energies and low absolute values of diffusivities.

The activation energies were correlated by two separate linear relations with the isosteric heats of adsorption, that is $E = 0.9q_{st}$ for nitrogen, argon, krypton, xenon, methane and benzene, and $E = 0.6q_{st}$ for ethylene, ethane, propylene, propane and n-butane. These relations might be used for the estimation of the activation energy. The obtained difference of the ratio of E to q_{st} is not explained here, but this might be the clue to interpreting the real mechanism of micropore diffusion in MSC in the future. Also, prediction of the preexponential factor of Arrhenius' equation will be of significance in future studies.

Molecular sieving carbon is comparable in two points with conventional molecular sieving materials such as zeolite and mordenite, which have network structure or straight pores. First, for the both adsorbents, MSC and zeolite, adsorbates are trapped at the points in the micropore where the potential energy is minimum. The potential energy distribution is ascribed to the interaction between adsorbate and lattice atoms surrounding the adsorbate. Second, diffusion of adsorbates occurs by traveling from site to site across the potential energy barrier.

Many investigations have been done for the static and dynamic adsorption on zeolite molecular sieves (Barrer, 1971; Ruthven and Derrah, 1975). But for molecular sieving carbons, there have been few works (Nelson et al., 1961; Walker et al., 1966). Kawazoe et al. (1971, 1974*b*) reported an extensive study of adsorption equilibrium characteristics of molecular sieving carbon. Also, diffusion in micropores of molecular sieving carbon was studied by Juntgen et al. (1975).

The authors (Kawazoe et al., 1974*a*) reported the chromatographic study of diffusion of nitrogen in the micropores of MSC for various surface coverages, and the concentration dependence of the diffusivity was explained in terms of chemical potential gradient as a driving force of diffusion.

This paper is concerned with the equilibrium and the rate of adsorption of various gases on molecular sieving carbon. Chromatographic measurements were made only for pure helium carrier, that is, nearly zero surface coverage of adsorbates. The various constants obtained will be attributed to the interaction between adsorbate and lattice forming atoms or carbon layer planes excluding the adsorbate-adsorbate interaction.

The theory of chromatography was modified here for taking into account the size distribution of microparticles.

METHOD OF ANALYSIS BY CHROMATOGRAPHY

The adsorption isotherm is given by a linear equation at near zero surface coverage:

$$q = K^* \cdot c \tag{1}$$

Under isothermal conditions, the differential equations which describe the change of concentration $c(t)$ in a packed bed of spherical particles with bidispersed pore structure and size distribution of the microparticles, such as the MSC employed here, are as follows:
Material balance in the bed

$$E_z \cdot \frac{\partial^2 c}{\partial z^2} - u\frac{\partial c}{\partial z} - \frac{3(1-\epsilon)}{\epsilon \cdot R} N_o = \frac{\partial c}{\partial t} \tag{2}$$

Material balance at the external surface of particles

$$N_o = k_f(c - c'|_{r_a=R}) = D_a \frac{\partial c'}{\partial r_a}\bigg|_{r_a=R} \tag{3}$$

Material balance in a particle

$$\frac{D_a}{\epsilon_a}\left(\frac{\partial^2 c'}{\partial r_a^2} + \frac{2}{r_a}\frac{\partial c'}{\partial r_a}\right) - \int_{-\infty}^{\infty} \frac{3(1-\epsilon_a)}{\epsilon_a \cdot a} \cdot \frac{\rho_p}{1-\epsilon_a} N_i(a) f(a) d\ln a = \frac{\partial c'}{\partial t} \tag{4}$$

Material balance at the surface of microparticles

$$N_i(a) = D\frac{\partial q}{\partial r_i}\bigg|_{r_i=a} \tag{5}$$

Adsorption equilibrium at the surface of microparticles

$$q = K^* \cdot c' \tag{6}$$

Material balance in the interior of a microparticle

$$D\left(\frac{\partial^2 q}{\partial r_i^2} + \frac{2}{r_i}\frac{\partial q}{\partial r_i}\right) = \frac{\partial q}{\partial t} \tag{7}$$

The resultant moment equations of the impulse response are

$$\mu_1 = \frac{z}{u}(1 + \delta_0) \tag{8}$$

$$\mu_2' = \frac{2z}{u}(\delta_d + \delta_f + \delta_a + \delta_i) \tag{9}$$

where

$$\delta_0 = \frac{(1-\epsilon)\epsilon_a}{\epsilon}\left(1 + \frac{\rho_p K^*}{\epsilon_a}\right) \tag{10}$$

$$\delta_d = \frac{E_z}{u^2}(1 + \delta_0)^2 \tag{11}$$

$$\delta_f = \frac{1-\epsilon}{\epsilon} \cdot \frac{R}{3k_f}(\epsilon_a + \rho_p K^*)^2 \tag{12}$$

$$\delta_a = \frac{1-\epsilon}{\epsilon} \cdot \frac{R^2}{15D_a}(\epsilon_a + \rho_p K^*)^2 \tag{13}$$

$$\delta_i = \frac{1-\epsilon}{\epsilon} \cdot \frac{\rho_p K^*}{15D}\int_{-\infty}^{\infty} a^2 f(a) d\ln a \tag{14}$$

The size distribution of the microparticles is assumed to be the log-normal distribution as

$$f(a) = \frac{1}{\sqrt{2\pi}\cdot\sigma}\exp\left[-\frac{(\ln a - \ln a_0)^2}{2\sigma^2}\right] \tag{15}$$

By introducing Equation (15) into Equation (14), we get

Fig. 1. Photomicrograph of the MSC pellet.

$$\delta_i = \frac{1-\epsilon}{\epsilon} \cdot \frac{\rho_p K^*}{15D}\bar{a}^2 \exp(\sigma^2) \tag{16}$$

δ_f is neglected for its small effects in the following analysis. For instance, by using Carberry's equation (Carberry, 1960), k_f can be estimated for the experimental condition. Then, the value of δ_f is found to be one order of magnitude smaller than δ_d or δ_a.

DETERMINATION OF MICROPARTICLE SIZE DISTRIBUTION FOR MSC 5A

The size distribution of the microparticles for MSC 5A was determined by the scanning electron microscope. By halving the MSC pellet, the crushed inner surface was photographed. A typical photomicrograph is shown in Figure 1. It is apparent that the macroparticle is an agglomerate of microparticles, and the microparticles have random shapes and size distribution. The diameters in the same orientation of about 100 microparticles were measured from three micrographs. On the assumption that the microparticle is a sphere, the cumulative number fraction was plotted against the microparticle radius a on a log-normal probability graph paper; a straight line was obtained as shown in Figure 2. It is assumed that microparticles of MSC 5A have the log-normal size distribution. The radius at the peak of the probability a_0', which corresponds to a number fraction basis, and the standard deviation σ were thus found to be 2.13 μ and 0.62, respectively. In the case of log-normal distribution, the straight lines of distribution both on number fraction basis and on volume fraction basis are parallel on a log-normal probability paper, and the

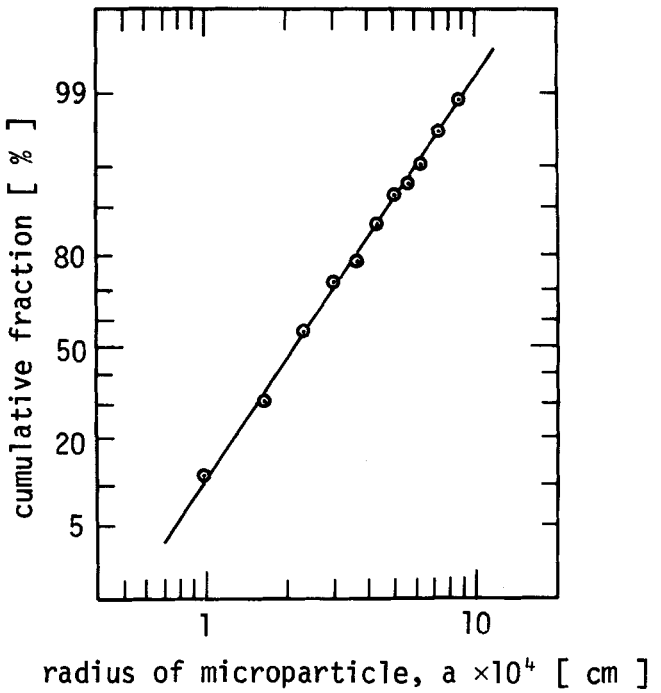

Fig. 2. Log-normal size distribution of the microparticles of MSC 5A.

TABLE 1. PROPERTIES OF MOLECULAR SIEVING CARBON (KAWAZOE ET AL., 1971)

Particle density, ρ_p (g/cm³)	0.90
True density (g/cm³)	1.8
Macropore volume (cm³/g carbon)	0.38
Micropore volume (cm³/g carbon)	0.18
Total pore volume (cm³/g carbon)	0.56
Porosity of macropore, ϵ_a	0.342
Macropore radius (μ)	2.0
Micropore opening (Å)	5

TABLE 2. PROPERTIES OF THE PACKED BED

Range of sieve openings [mm]	0.84-1.19
Average particle radius [mm]	0.50
Column diameter [mm]	3.0
Cross-sectional area of the column [cm²]	0.0707
Length of the packed bed [cm]	100
Mass of adsorbent [g]	3.46
Void fraction, ϵ	0.456
Column temp [°c]	−84-400°C
Carrier gas	He
Interstitial velocity, u [cm/s]	30-50

relation between the radius at the peak of the probability on a number fraction basis a_0' and that on a volume fraction basis a_0 is as follows (Hatch, 1933):

$$a_0 = a_0' \exp(3\sigma^2) \tag{17}$$

a_0 is 6.75 μ, and the arithmetic average radius $\bar{a}$ is 8.2 μ according to

$$\bar{a} = \frac{\int_{-\infty}^{\infty} af(a)d\ln a}{\int_{-\infty}^{\infty} f(a)d\ln a} = a_0 \exp\left(\frac{\sigma^2}{2}\right) \tag{18}$$

CHROMATOGRAPHIC MEASUREMENT

Experimental method was almost the same as the previous investigation (Kawazoe et al., 1974*a*). Carrier gas

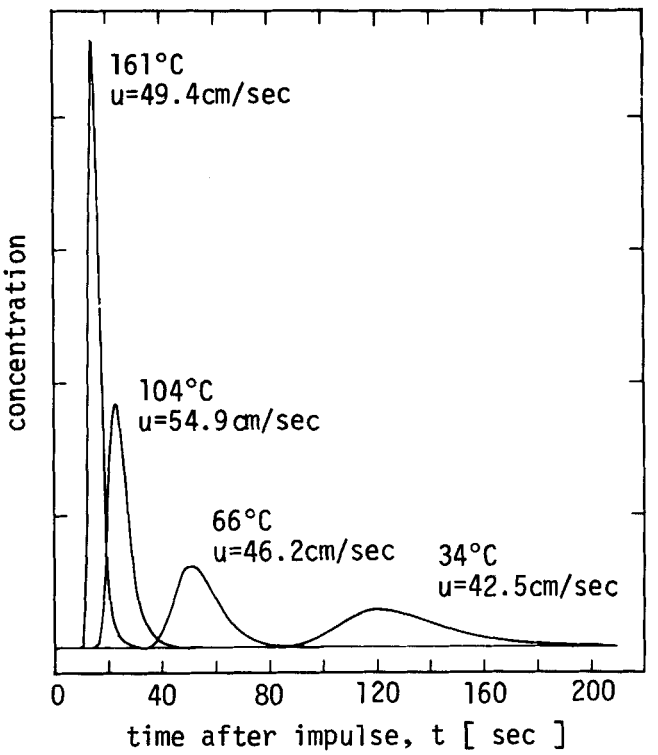

Fig. 3. Typical chromatographic peaks for krypton.

of the chromatograph was only helium in this study. Pulse volume was fixed to be 0.251 cm³.

The purities of the carrier gas (helium) and the sample gases are shown in Table 4.

The molecular sieving carbon was provided by Takeda Chemical Co. (MSC5A HGS 638). The properties of MSC5A are shown in Table 1. The original pellets were crushed and screened to yield the desired sizes of small particles. Before the runs, the bed of adsorbent particles was degassed by passing pure helium through the bed for 2 to 3 hr and vacuuming for 1 hr at 400°C.

The properties of the packed beds are shown in Table 2. The average particle diameter was taken as the arithmetic average of the maximum and minimum sieve openings. The porosities in the beds were estimated from bed volume, mass, and particle apparent density.

For each sample gas, runs were made at several temperatures, and at each temperature two interstitial velocities (about 45 and 33 cm/s) were chosen for measurement to check the contribution of axial dispersion.

The concentration of adsorbate in the effluent from the adsorbent bed was measured by the thermal conductivity cell. Figure 3 shows the effluent chromatographic peaks for krypton pulses at several temperatures for almost the same velocity.

The upper limit of the experimental temperature of certain gases was determined by the critical condition ($\rho_p K^* >> 1$). The lower limit of temperature studied here was determined by the relative magnitude of peak height and base line fluctuation at high sensitivity.

The first absolute moment and the second central moment were evaluated from the effluent peak $C_e(t)$ as follows:

$$\mu_1 = \int_0^{\infty} C_e(t)tdt / \int_0^{\infty} C_e(t)dt \tag{19}$$

$$\mu_2' = \int_0^{\infty} C_e(t)(t-\mu_1)^2 dt / \int_0^{\infty} C_e(t)dt \tag{20}$$

This information with Equation (9) allowed the contribu-

TABLE 3. TYPICAL DATA OF $\mu_1/(z/u)$ AND $\mu_2'/(2z/u)$ SHOWING CONTRIBUTION OF δ_d, δ_a, AND δ_i TO $\mu_2'/(2z/u)$ AND DEVIATION OF δ_i FROM THE AVERAGE OF TWO MEASUREMENT AT DIFFERENT VELOCITIES

Gas	Temp. [°C]	u [cm/s]	$\mu_1/(z/u)$	$\mu_2'/(2z/u)$ [s]	δ_d [%]	δ_a [%]	δ_i [%]	Error of δ_i [%]
CH_4	250	46.0	2.83	0.143	24.3	1.8	73.9	4.0
	100	46.9	12.4	4.00	16.4	4.7	78.9	4.1
	−19	45.8	229	2.07×10^3	11.1	6.8	82.1	—*
C_2H_4	307	48.1	5.15	0.839	13.7	1.7	84.5	—
	160	47.1	36.0	20.1	27.4	8.3	64.3	2.5
	62	46.7	489	3.18×10^3	32.1	15.9	52.0	18.1
C_2H_6	307	48.1	6.11	1.98	7.4	1.2	91.4	—
	160	48.6	51.8	102	10.8	3.7	85.6	8.7
	60	41.2	886	1.62×10^4	23.6	10.9	65.4	—
C_3H_6	400	43.8	7.29	2.26	8.4	1.4	90.3	—
	250	46.0	49.6	90.4	11.8	3.1	85.1	14.2
	160	47.1	414	2900	25.1	9.7	65.2	33.5
C_3H_8	394	46.2	7.23	11.8	2.3	0.3	97.5	—
	307	48.1	21.2	87.8	2.2	0.5	97.3	—
	250	46.0	54.2	403	3.2	0.9	95.9	6.2
nC_4H_{10}	393	46.2	18.7	86.6	1.7	0.4	97.9	56.7
	303	46.0	84.4	1.53×10^3	2.0	0.6	97.4	80.5
	235	44.8	375	1.49×10^4	5.4	1.3	93.3	—
C_6H_6	394	46.9	130	896	8.0	1.9	90.0	25.6
	380	42.4	193	2.46×10^3	7.4	1.5	91.1	—
	367	41.5	251	4.05×10^3	7.0	1.6	91.4	—
Ne	−84	41.0	1.82	3.6×10^{-2}	44.7	5.3	50.0	—
Ar	80	51.2	5.53	0.589	20.2	4.1	75.7	12.3
	26	44.2	8.49	2.50	13.0	4.5	82.4	15.1
	−19	45.8	24.1	26.6	10.0	5.1	85.0	—
Kr	161	49.4	6.17	1.27	12.1	2.4	85.5	5.9
	66	46.2	24.7	27.0	9.8	3.7	86.5	9.2
	−19	45.8	274	3.37×10^3	10.0	6.3	83.7	—
Xe	246	45.8	0.5	5.67	8.6	1.6	89.8	—
	163	38.5	33.0	51.6	11.4	2.7	85.9	—
	104	33.3	114	774	9.3	2.9	87.9	—
N_2	50	44.9	7.05	1.39	15.9	4.5	79.6	1.8
	26	44.2	9.29	3.12	12.5	4.6	82.9	20.9
	−18.2	45.9	28.8	36.9	9.8	5.4	84.8	—

* Measured at one velocity.

tion of axial dispersion and intraparticle diffusion to be evaluated separately.

The experimental first moment obtained by Equation (19) includes the effects of the volume of the pipe lines between the valve and the bed, 2.83 cm³, and that between the bed and detector, 1.32 cm³. This dead volume correction was first made for the experimental first moment μ_{1exp} to obtain the first moment for the bed itself μ_1 by using the equation

$$\mu_1 = \mu_{1exp} - \frac{2.83 + 1.32}{v} \qquad (21)$$

In Table 3, the upper and lower limits of the obtained moment data are shown as $\mu_1/(z/u)$ and $\mu_2'/(2z/u)$ corresponding to the experimental condition ranges of temperature and interstitial velocity.

The analysis of second moment was simplified by first dividing Equation (9) by $[\mu_1/(z/u)]^2$ obtained from Equation (8). The result was

$$H = \frac{\mu_2'}{\mu_1^2}\left(\frac{z}{2u}\right) = H_0 + \frac{E_z}{u^2} \qquad (22)$$

where

$$H_0 = \frac{\delta_a + \delta_i}{(1 + \delta_0)^2} \qquad (23)$$

E_z was expected to be proportional to u in the experimental condition. H_0 was able to be obtained as an intercept to the ordinate when H were plotted against $1/u$ according to Equation (22). Since δ_a could be estimated by the established evaluation equation for macropore diffusion and Equation (13), δ_i was obtained by Equation (23).

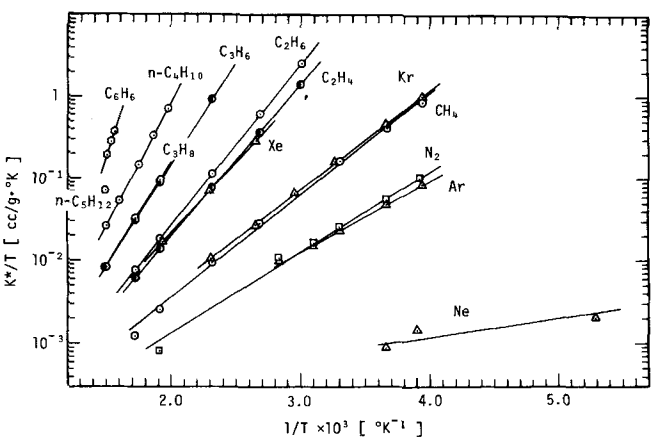

Fig. 4. Van't Hoff's plot of adsorption equilibrium constants.

ANALYSIS OF MOMENT DATA

Adsorption Equilibrium Constant

Equations (8) and (10) were used along with the μ_1 to obtain the adsorption constant K^*. The calculated values of K^* for two different velocities for each gas and temperature agreed with each other within 5% error. The isosteric heat of adsorption q_{st} is related with K^* for each

Table 4. Properties of Gases for Adsorption on MSC 5A and Purities of Gases

Gas	q_{st} [Kcal/mole]	$(K^*/T)_{1/T\to 0}$ [cm³/g · °K]	E [Kcal/mole]	D_0 [cm²/s]	α	Purity [mole or vol %]
CH_4	5.7	1.1×10^{-5}	4.8	1.3×10^{-4}	0.9	99.95 mole %
C_2H_4	8.5	3.9×10^{-6}	5.3	6.4×10^{-5}	0.6	99.5 mole %
C_2H_6	9.0	3.0×10^{-6}	5.5	2.3×10^{-5}	0.6	99.7 mole %
C_3H_6	11.4	1.6×10^{-6}	7.0	3.4×10^{-5}	0.6	99.7 mole %
C_3H_8	11.7	1.2×10^{-6}	7.0	6.8×10^{-6}	0.6	99.7 mole %
nC_4H_{10}	13.9	7.1×10^{-7}	7.8	3.0×10^{-6}	0.6	99.0 mole %
C_6H_6	21.8	1.3×10^{-8}	21.4	8.4×10^{-2}	0.9	99.5 chromato
Ne	1.1	1.1×10^{-4}	—	—	—	99.99 vol %
Ar	4.0	3.0×10^{-5}	3.9	1.7×10^{-4}	0.9	99.999 vol %
Kr	5.6	1.5×10^{-5}	4.8	8.4×10^{-5}	0.9	99.0 mole %
Xe	7.8	8.3×10^{-6}	6.5	7.2×10^{-5}	0.9	99.9 vol %
N_2	4.5	1.3×10^{-5}	3.9	1.5×10^{-4}	0.9	99.99 vol %
He						99.995 vol %

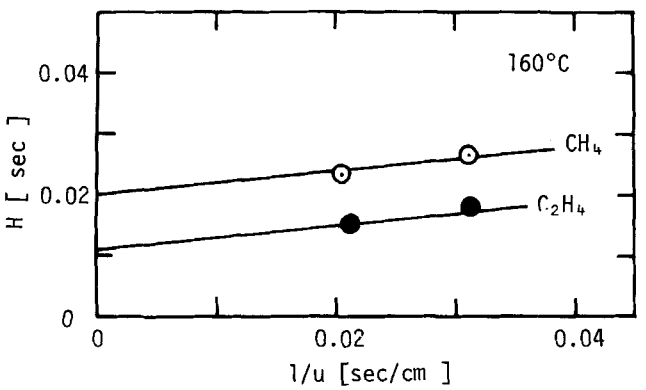

Fig. 5. Dependence of H on reciprocal velocity, $1/u$.

gas by Van't Hoff's equation:

$$\frac{K^*}{T} = \left(\frac{K^*}{T}\right)_{\frac{1}{T}\to 0} \exp\left(\frac{q_{st}}{R_g T}\right) \tag{24}$$

Here it is assumed that the gas is ideal.

According to Equation (24), the obtained K^* divided by T was plotted against $1/T$ for various gases in Figure 4, and the isosteric heat of adsorption q_{st} and $(K^*/T)_{1/T\to 0}$ were determined and listed in Table 4.

Axial Dispersion

Equation (22) shows that the contribution of axial dispersion to H must be evaluated first to estimate H_0 from experimental value of H. In packed beds, E_z is expressed as a sum of a molecular diffusion (D_M) term and a term due to the velocity profile

$$E_z = \frac{D_M}{\tau_{\text{ext}}} + \frac{d_p u}{Pe} \tag{25}$$

In this experiment, the particle size was 0.10 cm, and the values of $\epsilon d_p u/D_M$ were more than 1.0 for all runs. The second term of Equation (25) is expected to be dominant (Suzuki and Smith, 1971), and H in Equation (22) should depend linearly on $1/u$. Two examples are shown in Figure 5. By plotting all the data obtained the average Peclet number was evaluated from the gradient of the straight lines to be 0.50. This value was rather small in comparison with the empirical correlation (Suzuki and Smith, 1971) given as

$$Pe = 1.2\, d_p : d_p \text{ in mm} \tag{26}$$

but the same order of magnitude. There might be some channeling effect because the ratio of the tube diameter to the average particle size is 3.0, which is rather small compared with the figure used in ordinary experiments. The Peclet number thus obtained was used for all the runs to correct the contribution of axial dispersion and to obtain H_0. The percentage of the contribution of axial dispersion to $\mu_2'/(2z/u)$ was evaluated using Equations (9), (11), and (25) along with the obtained μ_1, μ_2', u, and Peclet number for each gas. These percentages were shown as $\delta_d(\%)$ in Table 3. The $\delta_d(\%)$, which means $1 - H_0/H$, was less than 30% for almost all the experiments, suggesting that the error introduced in this correction is relatively small.

Diffusion in Macropore

H_0 includes the effect of the macropore diffusion and the micropore diffusion.

The following established relation (Satterfield, 1970) was used to estimate the diffusivity in the macropore:

$$D_a = \frac{\epsilon_a}{\tau_p} \cdot D_M \tag{27}$$

The value of τ_p for MSC 5A was 3.2 in the previous work (Kawazoe et al., 1974*a*). Here, ϵ_a/τ_p was reasonably assumed as 0.1, and D_M was estimated by the equation of Hirschfelder et al. (1954). Equation (13) was then applied to estimate δ_a. Then, δ_i was obtained by Equation (23). The contribution of macropore diffusion and micropore diffusion to $\mu_2'/(2z/u)$ for each gas was evaluated and shown as $\delta_a(\%)$ and $\delta_i(\%)$ in Table 3. Throughout the experiment, $\delta_a(\%)$ was at most within 15% of $\mu_2'/(2z/u)$, so that the effect of the error induced from this estimation is also small. Table 3 also shows the error of δ_i, which is defined as the percentage of the difference between obtained δ_i and average δ_i to average δ_i for each gas.

Diffusion in Micropore

Since the size distribution of the microparticle for MSC 5A was already obtained by the electron microscope, diffusivities in micropores D were evaluated from δ_i, K^*, $\bar{a}$, and σ by using Equation (16). The values of D for different temperatures were plotted according to the following Arrhenius' equation in Figure 6:

$$D = D_0 \exp\left(-\frac{E}{RT}\right) \tag{28}$$

From Figure 6 the activation energy E was determined from the slope of the straight line corresponding to the data points for each gas; the preexponential factor D_0 was

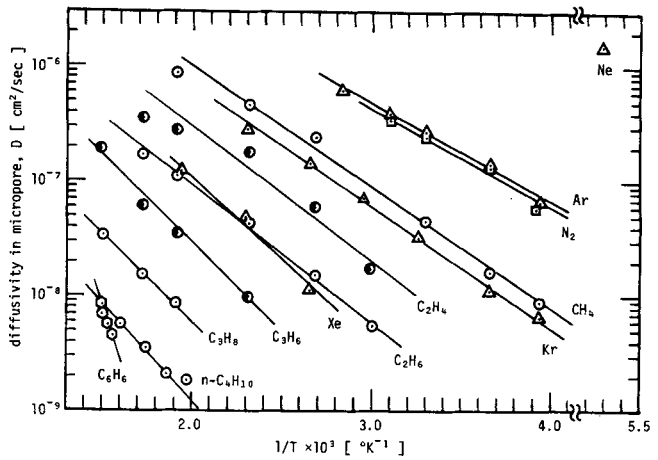

Fig. 6. Arrhenius' plot of diffusivities in micropore.

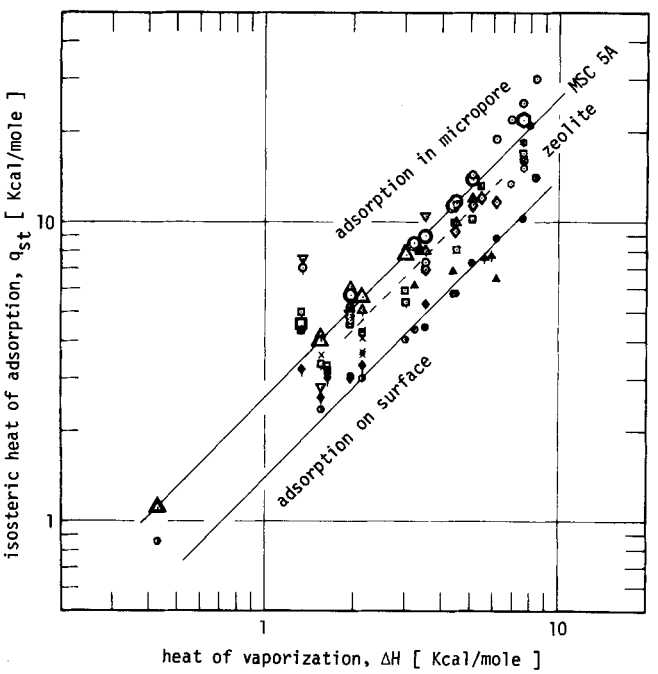

Fig. 8. Correlation of isosteric heat of adsorption with heat of vaporization.

ey	gas-solid	
○	n-paraffin	-MSC5A[this work]
○	n-olefin	
△	rare gas	
□	N_2	
○	benzene	
○	n-paraffin	-ColumbiaNXC(Hasz and Barrere,1969)
○	N_2	
■	n-paraffin & CF_4	-MS5A(Doetsh et al.,1974;Ruthven and Derrah,1972;Ruthven et al.,1973)
■	n-olefin	
▽	rare gas,O_2& N_2	-MS5A(Ruthven and Derrah, 1975)
○	paraffin	-MS13X(Ruthven and Doetsh, 1976)
●	aromatics	
▼	rare gas,O_2& N_2	-MS4A(Ruthven and Derrah, 1975)
●	paraffin & benzene	-MS13X(MacDonald and Habgood, 1972)
●	CH_4	-MS4A(Habgood, 1958)
×	Ar & Kr	-(Na-mordenite, H-mordenite) (Eberly, 1969)
△	n-paraffin	-H-mordenite(Mayorga and Peterson, 1972)
△	rare gas	
◇	paraffin	-zeolite L (Barrer and Lee, 1968)
▽	n-paraffin	-zeolite 4A(Eagan and Anderson, 1975)
▽	rare gas,N_2 & CO	
☆	n-paraffin	-HKT & NaY(Riekert, 1971)
●	n-paraffin	-GTCB(Kiselev and Poshkus, 1976)
●	n-olefin	
●	rare gas	-P-33(Sams et al., 1960)
●	n-paraffin	-porous glass(Barrer and Barrie, 1952)
↑	rare gas,N_2 & O_2	
▲	paraffin	-glass(Gilliland et al., 1974)
↑	inorganic gas	-glass,silica & carbon (Gilliland et al., 1974)

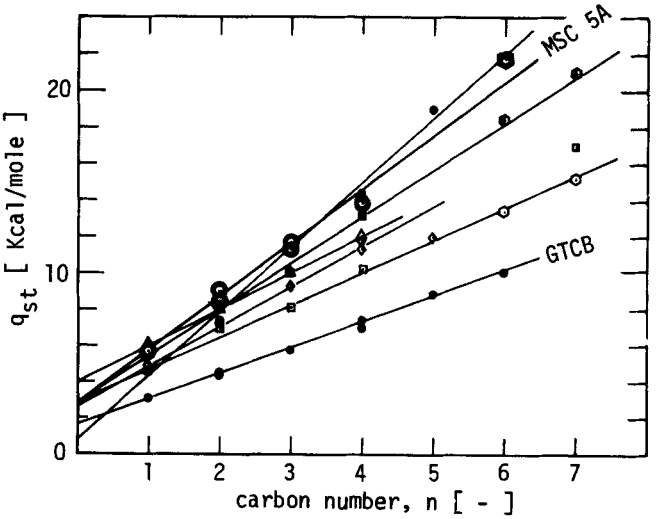

Fig. 7. Correlation of isosteric heat of adsorption with the carbon number *n* for hydrocarbons (keys refer to Figure 8).

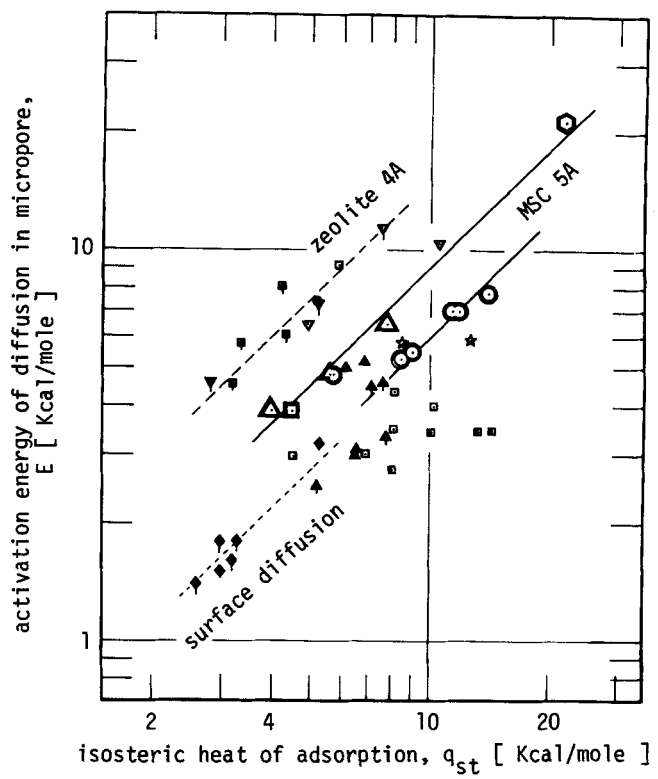

Fig. 9. Correlation of activation energy of the micropore diffusion with isosteric heat of adsorption (keys refer to Figure 8).

obtained as the interception to the ordinate at $1/T = 0$. Those figures were listed in Table 4.

DISCUSSION

Heat of Adsorption

The isosteric heat of adsorption obtained with the chromatographic method of MSC 5A in this study is characterized by two points. First, the estimated values are for zero coverage, or initial isosteric heats of adsorption. Therefore, these values correspond entirely to the interaction between the adsorbate molecule or atom and the adsorbent lattice atoms, excluding the interaction among adsorbate molecules. Secondly, the adsorbed molecules or atoms within the MSC 5A are held between two carbon layer planes of about 5Å opening. It is interesting to compare the values obtained here with the values for the case of

Table 5. α Values for Various Systems

Gas	Solid	α	Ref.
Ar, Kr, Xe, N_2, CH_4, C_6H_6	MSC 5A	0.9	This work
C_2H_4, C_2H_6, C_3H_6, C_3H_8, nC_4H_{10}	MSC 5A	0.6	This work
Ar, CO, N_2, CH_4, C_2H_6	MS 4A	1.5	Eagan and Anderson (1975)
Ar, Kr, O_2, N_2	MS 4A	1.5	Ruthven and Derrah (1975)
C_2H_4	Na Y	0.7	Riekert (1971)
n-C_5H_{12}	HKT	0.5	Riekert (1971)
O_2, N_2, Ar, Kr, CH_4, C_2H_6	Porous glass	0.6	Barrer and Lee (1968)
CO_2, SO_2, NH_3	Glass, silica and carbon	0.5-0.6	Gilliland et al. (1974)
C_2H_4, C_3H_6, iC_4H_{10}	Glass	0.5-0.8	Gilliland et al. (1974)

adsorption on carbon surfaces, such as on graphitized carbon blacks, and also with those for the adsorption in the zeolite cages or cylindrical pores.

The relations between the initial isosteric heats of adsorption q_{st} for hydrocarbons on MSC and the numbers of carbon atoms n of n-paraffin, n-olefin, and benzene are shown in Figure 7 with other investigator's data of q_{st} for hydrocarbons on other adsorbents. It should be noted that there exists a linear relation for MSC 5A; that is

$$q_{st} = 2.8 + 3.0\,n \tag{29}$$

The linear dependence of q_{st} for paraffins on carbon number n was first pointed out by Barrer and Lee (1968) for zeolite L. Also, the same correlation can be applicable to adsorption on activated carbon NXC (Hasz and Barrere, 1969), graphitized thermal carbon black (GTCB) (Kiselev and Poshkus, 1976), and Molecular Sieve 5A (Ruthven and Derrah, 1972; Ruthven et al., 1973; Doetsh et al., 1974; Ruthven and Derrah, 1975).

It is noted from Figure 7 that the initial heats of adsorption q_{st} for hydrocarbons on MSC 5A are approximately twice as much as those for hydrocarbons having the corresponding carbon number n on GTCB.

It should be noted from Figure 7 that the values of q_{st} of olefins on MS5A and aromatics on MS13X are fairly larger than those of paraffins having the corresponding carbon number n on MS5A and MS13X, but that the differences between the q_{st} values of olefins and paraffins having the same n are comparatively small in the case of MSC 5A or GTCB. This fact may be explained by the difference of affinities to nonpolar molecules between carbon base adsorbents and silicon-aluminum base adsorbents.

Including the data for all the other gases, q_{st} for MSC 5A are plotted against the heat of vaporization ΔH of adsorbates in Figure 8. Here again a linear relation can correlate all the data for MSC 5A (upper solid line in Figure 8):

$$q_{st} = 2.6\,\Delta H \tag{30}$$

Barrer and Lee (1968) showed that the ratios $q_{st}/\Delta H$ for zeolite L slightly exceeded 2. Other investigator's data for microporous adsorbents, such as activated carbon and zeolites, are plotted in Figure 8, where the ratio of $q_{st}/\Delta H$ is found to be between 2.0 and 3.0. The reported data of q_{st} in the case of adsorption on surface, such as those for GTCB (Kiselev and Poshkus, 1976) and porous glass (Barrer and Barrie, 1952), are also included in Figure 8, and the $q_{st}/\Delta H$ are found to range from 1.2 to 1.6.

These proportional relations of q_{st} to ΔH may be attributed to the fact that both q_{st} and ΔH are the parameters which represent the intermolecular forces. Furthermore, the difference between the $q_{st}/\Delta H$ for the adsorption in micropore and that on surface may be ascribed to the difference of the numbers of lattice atoms which interact with an adsorbed molecule for the both cases.

Activation Energy of the Micropore Diffusion

Diffusion in the micropore of the MSC is so called activated diffusion and is described as the molecules or atoms hopping from an adsorption site to another across the energy barrier which separates adjacent sites, which is similar to surface diffusion. The diffusion occurring between two carbon layer planes of MSC, however, is different from surface diffusion because a diffusing molecule interacts with the surrounding atoms of which the crystalline lattice consists. This may result in high absolute value of energy barrier compared with the potential energy of adsorption.

For MSC 5A, the obtained value of activation energy E was plotted against q_{st} in Figure 9. The two separate linear relations between E and q_{st} are observed:

$$E = \alpha \cdot q_{st} \tag{31}$$

The ratio of E to q_{st}, α, for rare gases, methane, and benzene is 0.9 and for n-paraffin except methane and n-olefin is 0.6. To explain this difference, more investigations will be needed in the future.

The data by other investigators are also shown in Figure 9, and α values determined by applying Equation (31) are listed in Table 5. Apparently a proportional relation exists also for diffusion in micropore of zeolite 4A with $\alpha = 1.5$. In the case of surface diffusion, the α values are about 0.5, and relatively small compared with diffusion in micropore.

CONCLUSION

Chromatographic measurements were made for various gas adsorptions on molecular sieving carbon at various temperatures, between $-84°$ and 400°C for zero coverage.

1. Adsorption equilibrium constants in the Henry's law region and diffusivities in the micropores in MSC were determined from the first absolute moment and the second central moment where the effects of all the other possible transport processes in the case of bidispersed pore structure and also the log-normal size distribution of the microparticle were taken into account.

2. The photographs of the microparticles of MSC by the scanning electron microscope exemplified the bidispersed pore structure and the log-normal size distribution of the microparticles.

3. The isosteric heats of adsorption were determined, and the linear relation was obtained with the carbon number

$$q_{st} = 2.8 + 3.0\,n$$

and with the heats of vaporization:

$$q_{st} = 2.6\,\Delta H$$

And the isosteric heats of adsorption on MSC were twice as much as those on graphitized thermal carbon black.

4. The activation energies of diffusion in the micropore of MSC were determined and found to be correlated by

two separate proportional relations to the isosteric heats of adsorption. For rare gases, methane, and benzene

$$E = 0.9\, q_{st}$$

and for n-paraffin and n-olefin except methane

$$E = 0.6\, q_{st}$$

NOTATION

a = radius of microparticle, cm
a_0 = a at the peak of the probability on a volume fraction basis, cm
a_0' = a at the peak of the probability on a number fraction basis, cm
$\bar{a}$ = arithmetic average radius of microparticles defined by Equation (18), cm
C_e = concentration in the effluent gas, mole/cm^3
c = concentration in the fluid phase, mole/cm^3
c' = concentration in the particle, mole/cm^3
D = diffusivity in micropores based on amount adsorbed gradient driving force, cm^2/s
D_0 = preexponential factor for the Arrhenius plot of D, cm^2/s
D_a = diffusivity in macropores, cm^2/s
D_M = molecular diffusivity, cm^2/s
d_p = particle diameter, cm
E = activation energy for micropore diffusion, Kcal/mole
E_z = axial dispersion coefficient based on void spaces in the bed, cm^2/s
$E_{z\cdot f}$ = dispersion coefficient due to fluid mixing, cm^2/s
$f(a)$ = distribution function of the radii of microparticles
H = defined by Equation (22), s
H_0 = defined by Equation (23), s
ΔH = heat of vaporization, Kcal/mole
K^* = adsorption equilibrium constant, cm^3/g
k_f = external mass transfer coefficient, cm/s
n = carbon number
N_i = flux at the surface of microparticle, mole · cm/g · s
N_o = flux at the external surface of particles, mole/cm^2 · s
Pe = Peclet number, $d_p u/E_{z\cdot f}$
q = amount adsorbed per unit mass of adsorbent, mole/g
q_{st} = isosteric heat of adsorption, Kcal/mole
R = radius of particles, cm
R_g = gas constant, Kcal/mole · °K
r_a = radial position in a particle, cm
r_i = radial position in a microparticle, cm
T = absolute temperature, °K
t = time, s
u = interstitial velocity of fluid, cm/s
v = volumetric flow rate, cm^3/s
z = longitudinal position in the bed, cm

Greek Letters

α = ratio of E to q_{st}
$\delta_0, \delta_a, \delta_i, \delta_d, \delta_f$ = defined by Equations (10) to (14)
ϵ = void fraction in the bed
ϵ_a = macropore fraction in the particle
μ_1 = first absolute moment of the chromatographic peak, s
μ_2' = second central moment, s^2
ρ_p = particle density, g/cm^3
σ = standard deviation defined by Equation (15)
τ_{ext} = tortuosity factor of interstitial fluid path
τ_p = tortuosity factor of macropores

LITERATURE CITED

Barrer, R. M., "Intracrystalline Diffusion," *Adv. Chem.*, **102**, 1 (1971).

——— and J. A. Lee, "Hydrocarbons in Zeolite L," *Surface Sci.*, **12**, 341 (1968).

Barrer, R. M., and J. A. Barrie, "Sorption and Surface Diffusion in Porous Glass," *Proc. Royal Soc. London*, **A213**, 250 (1952).

Carberry, J. J., "A Boundary-Layer Model of Fluid-Particle Mass Transfer in Fixed Beds," *AIChE J.*, 6, 460 (1960).

Doetsh, I. H., et al., "Sorption and Diffusion of n-Heptane in 5A Zeolite," *Can. J. Chem.*, **52**, 2727 (1974).

Eagan, J. D., and R. B. Anderson, "Kinetics and Equilibrium of Adsorption on 4A Zeolite," *J. Colloid Interface Sci.*, **50**, No. 3, 419 (1975).

Eberly, P. E., Jr., "Diffusion Studies in Zeolites and Related Solids by Gas Chromatographic Techniques," *Ind. Eng. Chem. Fundamentals*, 8, No. 1, 25 (1969).

Gilliland, E. R., et al., "Diffusion on Surface. I. Effect of Concentration on the Diffusivity of Physically Adsorbed Gases," *ibid.*, **13**, No. 2, 95 (1974).

Habgood, H. W., "The Kinetics of Molecular Sieve Action. Sorption of Nitrogen-Methane Mixtures by Linde Molecular Sieve 4A," *Can. J. Chem.*, **36**, 1384 (1958).

Hasz, J. W., and C. A. Barrere, Jr., "Prediction of Equilibrium Adsorption Capacity and Heats of Adsorption by the Polanyi Potential Theory," *Chem. Eng. Progr. Symposium Ser., No. 96*, **65**, 48 (1969).

Hatch, T., "Determination of "Average Particles Size" from the Screen-Analysis of Non-Uniform Particulate Substances," *J. Franklin Inst.*, **215**, No. 1, 27 (1933).

Hirschfelder, J. O., et al., *Molecular Theory of Gases and Liquids*, Wiley, New York (1954).

Juntgen, H., et al., "Diffusion von Gasgemischen durch Engstellen als geschwindigkeitsbestimmender Schritt der Porendiffusion in Kohlenstoffhaltigem Material," *Ber. Bunsen-Ges. Physik. Chem.*, **79**, 824 (1975).

Kawazoe, K., et al., "Adsorption Equilibrium on Molecular Sieving Carbon," *Kagaku Kogaku*, 35, No. 9, 1006 (1971).

———, "Chromatographic Study of Diffusion in Molecular-Sieving Carbon," *J. Chem. Eng. Japan.*, **7**, No. 3, 151 (1974 *a*).

———, "Correlation of Adsorption Equilibrium Data of Various Gases and Vapors on Molecular-Sieving Carbon," *ibid.*, 158 (1974 *b*).

Kiselev, A. V., and D. P. Poshkus, "Molecular-statistical Calculation of the Thermodynamic Characteristics of Adsorption of Saturated and Unsaturated Hydrocarbons on Graphitized Thermal Carbon Black," *J. C. S. Faraday Trans. I.*, **72**, 950 (1976).

MacDonald, W. R., and H. W. Habgood, "A Gas Chromatographic Method for the Determination of Masstransfer Resistances in Zeolite Catalysis," *Can. J. Chem. Eng.*, **50**, 462 (1972).

Mayorga, G. D., and D. L. Peterson, "Adsorption in Mordenite. II. Gas Chromatographic Measurement of Limiting Heats of Adsorption of Nonpolar Molecules," *J. Phys. Chem.*, **76**, No. 11, 1647 (1972).

Nelson, E. T., and P. L. Walker, Jr., "Some Techniques for Investigating the Unsteady-state Molecular Flow of Gas Through a Microporous Medium," *J. Appl. Chem.*, **11**, 358 (1961).

Riekert, L., "Rates of Sorption and Diffusion of Hydrocarbons in Zeolites," *AIChE J.*, 17, No. 2, 446 (1971).

Ruthven, D. M., and R. I. Derrah, "Transition State Theory of Zeolitic Diffusion, Diffusion of CH_4 and CF_4 in 5A Zeolite," *J. C. S. Faraday Trans. I.*, **68**, 2332 (1972).

Ruthven, D. M., et al., "Diffusion of Light Hydrocarbons in 5A Zeolite," *Can. J. Chem.*, **51**, 3514 (1973).

Ruthven, D. M., and R. I. Derrah, "Diffusion of Monatomic and Diatomic Gases in 4A and 5A Zeolites," *J. C. S. Faraday Trans. I.*, **71**, 2031 (1975).

Ruthven, D. M., and I. H. Doetsch, "Diffusion of Hydrocarbons in 13X Zeolite," *AIChE J.*, **22**, No. 5, 882 (1976).

Sams, J. R., Jr., et al., "Second Virial Coefficients of Neon, Argon, Krypton and xenon with a Graphitized Carbon Black," *J. Phys. Chem.*, **64**, 1689 (1960).

Satterfield, C. N., *Mass Transfer in Heterogeneous Catalysis*, p. 33, M.I.T. Press, London, England (1970).
Suzuki, M., and J. M. Smith, "Axial Dispersion in Beds of Small Particles," *Chem. Eng. J.*, 3, 256 (1971).
Walker, P. L., Jr., et al., "Activated Diffusion of Gases in Molecular Sieve Materials," in *Chemistry and Physics of Carbon* 2, pp. 257-371, Dekker, New York (1966).

Manuscript received June 7, 1977; revision received October 14 and accepted October 27, 1977.

Interfacial Resistance to Interphase Mass Transfer in Quiescent Two-Phase Systems

HOWARD BRENNER
and
L. GARY LEAL
Department of Chemical Engineering
California Institute of Technology
Pasadena, California 91125

Interfacial resistance to solute mass transfer between two unstirred immiscible fluids is theoretically calculated. Solute molecules are modeled as Brownian particles, bathed by homogeneous fluid continua when wholly immersed in either fluid, or else by heterogeneous fluid continua when instantaneously straddling the interface. These diffusing particles are assumed to be subjected to either repulsive or attractive conservative forces exerted on them by the interface. Additionally, their mobility is supposed affected by proximity to the interface. Circumstances are found to exist under which the interface may offer significant resistance to interphase transport. Surprisingly, conditions also exist in which the interface may actually offer a negative resistance to such solute transfer. In such cases, the presence of the interface enhances the overall interphase mass transfer rate.

SCOPE

Solute mass transfer between two immiscible fluids is of fundamental importance in a variety of industrial operations and research activities. Little is known, however, of the resistance offered by the interface itself to solute transfer across it, except that it can be appreciable in some systems (Davies and Rideal, 1963; Chandrasekhar and Hoelscher, 1975) compared with that offered by the individual bulk fluids. This paper reports upon a theoretical study of interphase mass transfer in a quiescent unstirred system, across which a steady concentration gradient is maintained, normal to the interface. This represents the simplest class of such transport problems.

The diffusing solute molecules are modeled as spherical Brownian particles, subject to external forces exerted on them by the interface. Independently, their Brownian diffusivity is decreased by their relative proximity to the interface. Such anomalous effects are important only in the domain extending several sphere radii a on either side of the interface. Beyond this region, ordinary unhindered bulk diffusion concepts apply. In this sense, the anomalous region immediately surrounding the interface plays the role of a transition layer, smoothly and continuously joining together the otherwise discontinuous bulk properties associated with the particles in each of the two fluids bounding the layer.

Local equilibrium is not assumed to exist at the interface. Indeed, at the microscopic level of description of the problem, appropriate to an observer able to resolve concentration variations on length scales of order a, the solute concentration varies continuously across the interface, from one bulk value to the other. As such, the conventional concept of interphase solute equilibrium is devoid of meaning. Rather, the concept is meaningful only at a macroscopic or bulk level, corresponding to a macroscopic length scale $L >> a$. Viewed from this length scale, the local solute concentration will appear discontinuous across the interface. The origin of interfacial resistance, which is a macroscopic concept, resides in viewing particle transport through the transition region from the vantage point of a macroscopic observer at the length scale L.

The object of this investigation consisted of developing a quantitative theory of the phenomenon, in which the resistance offered by the interface itself could be related to the fundamental microscopic physical parameters of the system, namely, the potential energy function characterizing the repulsive and/or attractive forces and the position-dependent particle diffusivity.

CONCLUSIONS AND SIGNIFICANCE

The interfacial resistance to solute mass transfer across a two-fluid layer of specified thickness $L = L_1 + L_2$ was defined as the difference between the overall resistance and the sum of the diffusional resistances of the individual bulk fluid layers of thicknesses L_1 and L_2, respectively. This led ultimately to a quantitative expression for the interfacial resistance containing two parametric functions: the position-dependent potential energy function, governing the repulsive or attractive forces exerted on the Brownian solute molecules by the interface, and the variation of the Brownian diffusion coefficient with distance of the sphere center from the interface.

Correspondence concerning this paper should be addressed to Howard Brenner, Department of Chemical Engineering, University of Rochester, Rochester, New York 14627.

0001-1541-78-1004-0246-$01.15.